Preprint YERPHI-1388(33)-91

ԵՐԵՎԱՆԻ ՖԻԶԻԿԱՅԻ ԻՆՍՏԻՏՈՒՏ
ЕРЕВАНСКИЙ ФИЗИЧЕСКИЙ ИНСТИТУТ
YEREVAN PHYSICS INSTITUTE

S.I. KARABEKIAN, S.G.ODOULOV*

BULK PHOTOVOLTAIC EFFECT IN $LiTaO_3$:Fe CRYSTALS

29-42

ЦНИИатоминформ
ЕРЕВАН - 1991

We regret that some of the pages in this report may not be up to the proper legibility standards, even though the best possible copy was used for scanning

Նախնատիպ ԵՖԻ-1388(33)-91

Ա.Ի. ԿԱՐԱԲԵԿՅԱՆ, Ս.Գ. ՕԴՈՒԼՈՎ*

ԾԱՎԱԼԱՅԻՆ ՖՈՏՈՎՈԼՏԱԻԿ ԷՖԵԿՏԸ $LiTaO_3$:Fe ԲՅՈՒՐԵՂՈՒՄ

Առանց սիմետրիայի կենտրոնի բյուրեղներում առաջացող ծավալային ֆոտովոլտաիկ էֆեկտը որոշվում է երրորդ կարգի թենզորով։ Աշխատանքում առաջին անգամ $LiTaO_3$:Fe բյուրեղի համար չափվել են գծային ֆոտովոլտաիկ էֆեկտի թենզորի բոլոր չորս անկախ բաղադրիչները և բերվել են նրանց սպեկտրալ կախվածությունները ֆոտոնների 2.07էՎ-3.88էՎ էներգիաների տիրույթում։ β_{15} և β_{22} բաղադրիչների սպեկտրալ կախվածությունների կոռելյացիայի հիման վրա հետևություն է արվել այդ նյութում լայնակի ֆոտովոլտաիկ հոսանքների ընդհանուր ծագման վերաբերյալ։

Երևանի ֆիզիկայի ինստիտուտ

Երևան 1991

---

*Ուկրաինական ՍՍՀ Գիտ. Ակադ. ֆիզիկայի ինստիտուտ

1. Introduction

In noncentrosymmetric crystals, at their homogeneous illumination there arises a steady-state current [1]. According to the phenomenological theory [2] the expression of the photovoltaic current density has the form:

$$j_i = \beta_{inl} E_n E_l^* + i\gamma_{il} [EE^*]_l , \qquad (1)$$

where E_n, E_l are the components of electric field of the light wave, β_{inl} and γ_{il} are the components of symmetric third-rank tensor and the second-rank pseudotensor, respectively. The first term in this expression relates the photovoltaic current density to the field of linearly polarized wave, and is called "linear photovoltaic current". The second term is nonvanishing for elliptically polarized wave only and is called "circular photovoltaic current".

For 3-m point group crystals, to which $LiTaO_3$:Fe belongs, the third-rank tensor β_{in} has four independent nonvanishing components: β_{33}, β_{31}, β_{22} and β_{15}. The linear photovoltaic currents are:

$$\begin{aligned} j_x &= \beta_{22}(E_x E_y^* + E_x^* E_y) + \beta_{15}(E_x E_z^* + E_x^* E_z) , \\ j_y &= \beta_{22}(E_x E_x^* + E_y^* E_y) + \beta_{15}(E_y E_z^* + E_y^* E_z) , \\ j_z &= \beta_{31} E_x E_x^* + \beta_{31} E_y E_y^* + \beta_{33} E_z^* E_z . \end{aligned} \qquad (2)$$

There are nine possible experimental geometries to measure β_{inl}, where the light propagates along one of the crystallographic axes and the current is also measured along the same or other crystallographic axes. The expressions for photovoltaic current density for each of the nine situations are presented in Table 1 [4].

The linear photovoltaic effect was earlier studied in $LiNbO_3$:Fe, Cu [1,3-5], $LiTaO_3$ [6] and $LiTaO_3$:Cu samples [7].

The results of measurement of all four independent components of the linear photovoltaic effect in $LiTaO_3$:Fe crystals are presented in this work for the first time. One of the goals of this study is to establish whether the same photovoltaic centers are responsible for all the components of the linear photovoltaic effect in this material. With this purpose the spectral dependences for different photovoltaic currents are measured.

By the technique suggested in [7] and [5] we obtain data on β^S_{15} symmetric non-diagonal component of the linear photovoltaic effect. On the basis of correlation of the spectral dependences of β^S_{15} and β_{22} components we conclude that most probably, the same centers are responsible for different transverse photovoltaic currents in this material.

2. The Experimental Technique

2.1. Experimental Setup

The schematic drawing of the experimental arrangement for photovoltaic current measurements is analogous to that described in Ref.[4]. A 1kW xenon lamp was used as a source of light. The light was monochromated by means of a СФ-26 spectrometer, then polarized by a polarizer, and focused on the crystal. The crystal was mounted on a measuring head (Fig.1) which could be turned independently in two mutually perpendicular planes, with the help of a remote control. The head with the samples, in its turn, was placed in a shielded and heat-insulated vessel. The contacts were made by vacuum deposition of silver. The photovoltaic current was measured by an electrometer.

The $LiTaO_3$:Fe samples (0.038wt.%) were poled by application of 0.3V/cm electric field during 15 minutes in a H_2 atmosphere at 700°C. The measurements were carried out on

$LiTaO_3$:Fe crystals measuring X:Y:Z=2.75:4.8:4.25mm^3. The orientation of the sample faces to the crystallographic axes was up to 10 angular seconds. All the results obtained were corrected with regard to the absorption and non-uniformity of the crystal illumination, according to the technique proposed in Ref.[4]. The spectral dependences of the absorption coefficients for ordinary and extraordinary waves are shown in Fig.2. The measuring accuracy of the ratio of the photovoltaic current to intensity is estimated to be no more than ±13%, and at measuring the absorption coefficients - no more than ±2%.

2.2. Measurement of β_{15} Photovoltaic Tensor Component

As far as $LiTaO_3$:Fe is a single-axis crystal, the speed of propagation of ordinary and extraordinary waves in it will be different. As follows from Eq.(2), when the light is propagating along OY axis and the incident light wave is polarized at 45^o with respect to OZ and OX axes, the photovoltaic currents along OX axis, determined by the tensor component β_{15}, will oscillate in space with a period of $\Lambda=\lambda/(n_o-n_e)$ (λ is the light wavelength, n_o and n_e are ordinary and extraordinary refraction indices, respectively). A method proposed earlier in [7] was used in this work to measure the currents determined by the β_{15} component. The essence of the method is the following: if the XOY face of the crystal is exposed to light at an angle lying in the XOZ plane and polarized in the same plane (Fig.3), then only an extraordinary wave will propagate in the crystal, the vector of the electric field of which will have non-zero components along both X and Z axes. The photovoltaic current along X axis will contain a spatially uniform component, which is defined by the expression

$$j_x = \beta_{15} I^{(t)} \sin 2\alpha , \qquad (3)$$

where $I^{(t)}$ is the intensity of light in the sample, α is the

angle between the direction of propagation of light and Z axis in the sample. The intensity of the light in the sample is: $I^{(t)}=I(1-R_{\parallel})$, where $R_{\parallel}=\tan^2(\alpha^0-\alpha)/\tan^2(\alpha^0+\alpha)$ is reflectivity of crystal face , I is the intensity of incident light; $\alpha=\arcsin((\sin\alpha^0)/n_e)$, α^0 is the angle of incidence. The measuring head was rotated in the XOZ plane to measure the angular dependence of the photovoltaic current density j_x.

3. Experimental Results and Discussion

Three of the nine polarization dependences of photovoltaic current density for photon energy of exciting light 2.6eV are presented in Fig.4. These dependences agree perfectly well with the theoretical predictions given in Table 1, which allows us to calculate by them the values of β_{31}, β_{33} and β_{22} for given quantum energy.

The angular dependence of photovoltaic current density along X axis is shown in Fig.5. It also fits quite well to the expression (3). When turning the sample around X axis by 180^0, the current determined by β_{15} component changes its sign, this also being in agreement with the proposed model.

When measuring the spectral dependence of β_{15}, we measured the first angular dependence of j_x for several photon energies, and the value of β_{15} was calculated from the slope of each angular dependence according to the formula (3). In the same manner the dependence of photovoltaic current density on the light intensity was obtained.

Fig.6 represents the light intensity dependence for photovoltaic currents due to β_{31},β_{33}, β_{15} and β_{22} tensor components. All four dependences are linear, in agreement with the phenomenological expression (1).

The spectral dependences for photovoltaic tensor components are shown in Fig.7. When comparing the results obtained, one may notice that all the components grow with increasing photon energy of incident light. With increasing

photon energy β_{31} becomes larger than β_{33}, like in the case with a $LiNbO_3$:Fe crystal [4]. But, as distinct from $LiNbO_3$:Fe, β_{15}^{s} in $LiTaO_3$:Fe has a larger absolute value than β_{22}.

In the energy range from 2.1eV to 4.0eV, for $LiTaO_3$:Fe (0.038 wt%) β_{33}, β_{15}, β_{22} normalized to β_{31} are $\beta_{21}/\beta_{31}=(3.1\pm1.7)10^{-2}$; $\beta_{15}/\beta_{31}=(6.7\pm5.2)10^{-2}$; $\beta_{33}/\beta_{31}=1\pm0.35$.

According to Glass et al. [1], the ratio J/I is defined as:

$$J/I = k\alpha = \frac{pL\alpha e}{\hbar\omega} = \mu\tau E_{ph}\frac{\alpha e}{\hbar\omega},$$

where k is the Glass constant, p is quantum efficiency, L is the mean free path, μ is mobility, τ is the time in which the excited carriers contribute to the anisotropic charge transport, E_{ph} is a phenomenologically introduced local field acting on the charge carriers.

A characteristic feature of the spectral dependence of β_{33}, β_{22} and β_{15} components is the presence of a shoulder in the energy range from 2.1eV to 2.7eV. To make a detailed analysis of the spectral dependence of the tensor components possible, in Fig.8a are presented the spectral dependences of the ratio of β_{33}, β_{22} and β_{15} to β_{31}, the spectrum of which contains no sharp features. Fig.8b presents the similar ratios of k_{33}, k_{15} and k_{22} constants to k_{31}. It is seen from Fig.8, that the ratio of β_{33}/β_{31} depends on the quantum energy least of all (is independent of the quantum energy with an accuracy of up to 35%). The growth of k_{33}/k_{31} with decreasing photon energy is due to the difference in the spectral dependence of the absorption coefficient for ordinary and extraordinary waves. The ratios of the Glass constants k_{15}/k_{31} and k_{22}/k_{31} coincide by definition with the ratios β_{15}/β_{31} and β_{22}/β_{31}, respectively. Fig.8 shows an obvious correlation between the spectral dependences of β_{15}/β_{31} and β_{22}/β_{31}. The curves qualitatively recur in shape. The maximum and minimum points correspond to the same energy of incident light. Such a correlation allows us to assume that the photovoltaic currents

that propagate in a direction perpendicular to $\vec{C}$ axis in $LiTaO_3$:Fe arise due to photoexcitation of carriers from the same admixture or defect centers.

We now try to juxtapose the data available on photovoltaic constants of doped crystals of 3m-point group. Table 2 contains photovoltaic constants for $LiNbO_3$:Fe, $LiNbO_3$:Cu crystals taken from Ref.[4], the values for $LiNbO_3$:Fe partly published in [5], and the values measured in the present work for $LiTaO_3$:Fe, all at quantum energy 3eV. The discrepancy of data for $LiNbO_3$:Fe [4,5] (which is less than 70% in case of k_{33}) may be due to the peculiarities of the reduction process for samples of different origin.

As is seen from Table 2, the Glass constants k_{22}, k_{15} and the product of quantum efficiency by mean free path $(pL)_{22}$, $(pL)_{15}$ for $LiTaO_3$:Fe are several times smaller than the same values for $LiNbO_3$:Fe. It should be also noted, that the photovoltaic constants k_{15}, $(pL)_{15}$ in $LiTaO_3$:Fe crystals are larger than the constants k_{22}, $(pL)_{22}$.

In conclusion the authors express their gratitude to Dr. I.N.Kiseleva and Dr. K.G.Belabaev for providing the $LiTaO_3$:Fe samples.

Table 1

Polarization dependences of photovoltaic currents for different directions of light propagation.

direction of current	direction of propagation of light		
	X	Y	Z
X	0	$\beta_{15} I \sin 2\theta$	$-\beta_{22} I \sin 2\theta$
Y	$\beta_{15} I \sin 2\theta$ + $+ \beta_{22} I \cos^2\theta$	$-\beta_{22} I \cos^2\theta$	$\beta_{22} I \cos 2\theta$
Z	$\beta_{31} I$ + $+ (\beta_{33}-\beta_{31}) I \cos^2\theta$	$\beta_{31} I$ + $+ (\beta_{33}-\beta_{31}) I \cos^2\theta$	$\beta_{31} I$

θ is the angle between the directions of polarization of light and measurement of current. In case of *yy*, θ is the angle between the light polarization vector and X axis.

Table 2

Photovoltaic constants	$LiNbO_3$:Fe [4]	$LiNbO_3$:Fe [5]	$LiNbO_3$:Cu [4]	$LiTaO_3$:Fe
k_{31} cmV^{-1}	$3.3 \cdot 10^{-9}$	$4.3 \cdot 10^{-9}$	$1.0 \cdot 10^{-9}$	$2.8 \cdot 10^{-9}$
$(pL)_{31}$ Å	1.0	1.3	0.3	0.84
k_{33} cmV^{-1}	$2.7 \cdot 10^{-9}$	$4.8 \cdot 10^{-9}$	$0.6 \cdot 10^{-9}$	$3.2 \cdot 10^{-9}$
$(pL)_{33}$ Å	0.8	1.4	0.2	1.0
k_{22} cmV^{-1}	$0.3 \cdot 10^{-9}$	$0.36 \cdot 10^{-9}$	$0.07 \cdot 10^{-9}$	$0.05 \cdot 10^{-9}$
$(pL)_{22}$ Å	0.08	0.11	0.02	0.015
k_{15} cmV^{-1}	-	$0.21 \cdot 10^{-9}$	-	$0.07 \cdot 10^{-9}$
$(pL)_{15}$ Å	-	0.06	-	0.02

Figure Captions

Fig.1 Schematic representation of the exerimental arrangement.: Measuring head (A) with crystal (B) inside it can be turned around two axes, as shown by arrows.

Fig.2 Absorption spectrum for $LiTaO_3$:Fe (0.038 wt.%).

Fig.3 Experimental geometry for β_{15} mesasurement.

Fig.4 Photovoltaic current density versus polarization angle at 2.6 eV. Solid lines represent the best fit to the calculated dependeces, $j_x/I=-\beta_{22}\sin 2\theta$, $j_y/I=\beta_{22}\cos 2\theta$ and $j_z/I=\beta_{31}+(\beta_{33}-\beta_{31})\cos^2\theta$. In each curve θ is the angle between polarization vector and crystallographic axis.

Fig.5 Angular dependence of the photovoltaic c ent density j_x for photon energy 2.6 eV.

Fig.6 The light intensity dependence for diffe nt components of photovoltaic current density (determined by four photovoltaic tensor components) for photon energy 2.6 eV.

Fig.7 Spectra of photovoltaic tensor components for $LiTaO_3$:Fe (0.038 wt.%).

Fig.8 Spectra of photovoltaic tensor component ratios (a) and of the Glass constant ratios (b) in $LiTaO_3$:Fe (0.038 wt.%).

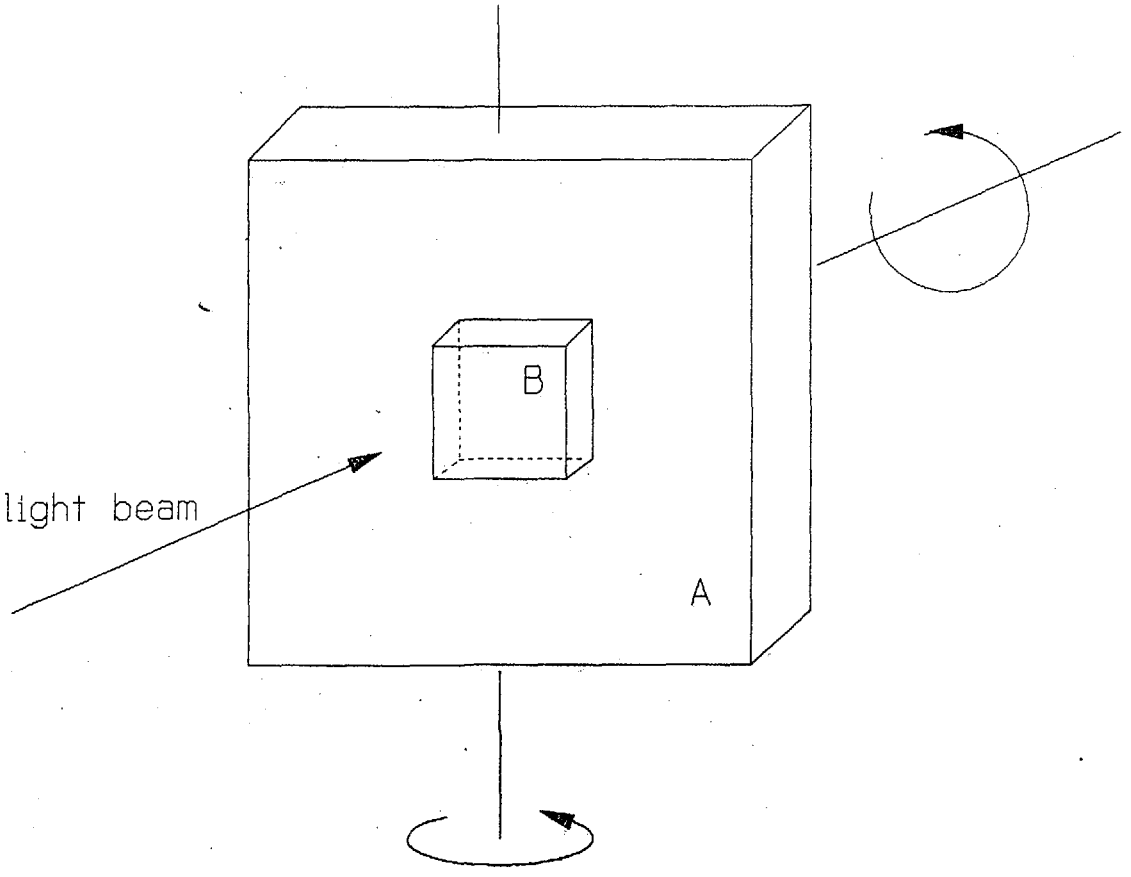

Fig.1

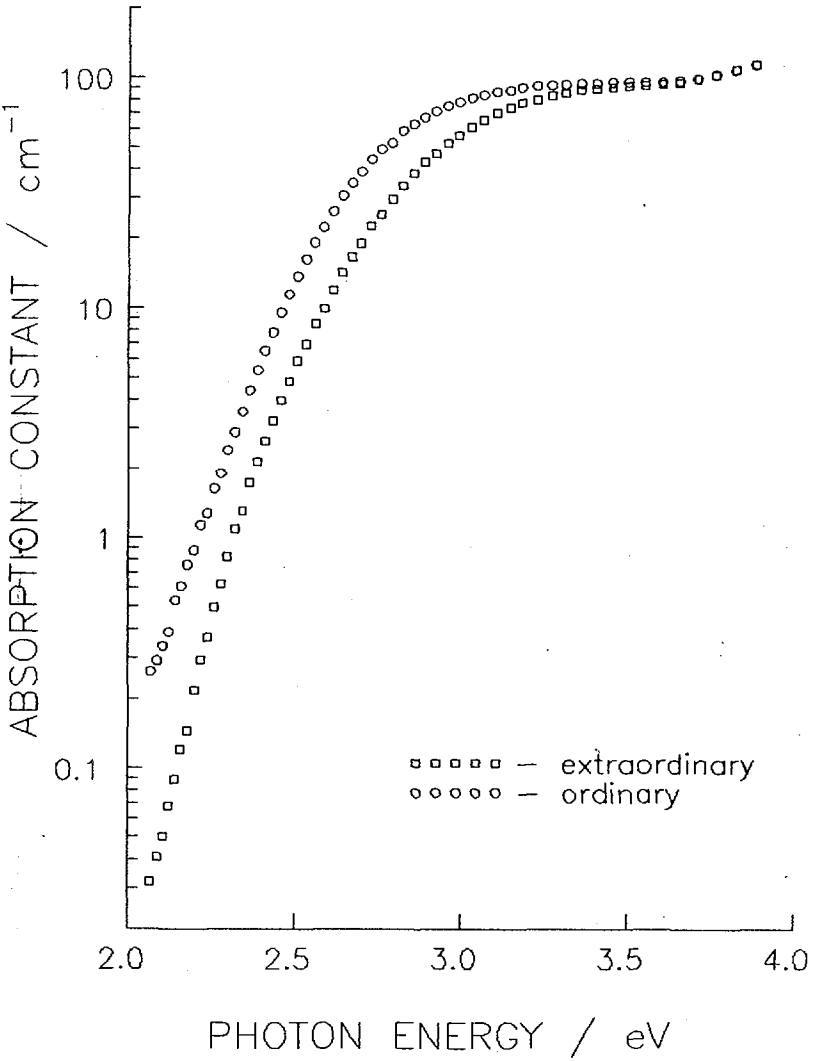
ABSORPTION CONSTANT / cm^{-1}
100
10
1
0.1
2.0
2.5
3.0
3.5
4.0
PHOTON ENERGY / eV
extraordinary
ordinary

Fig.2

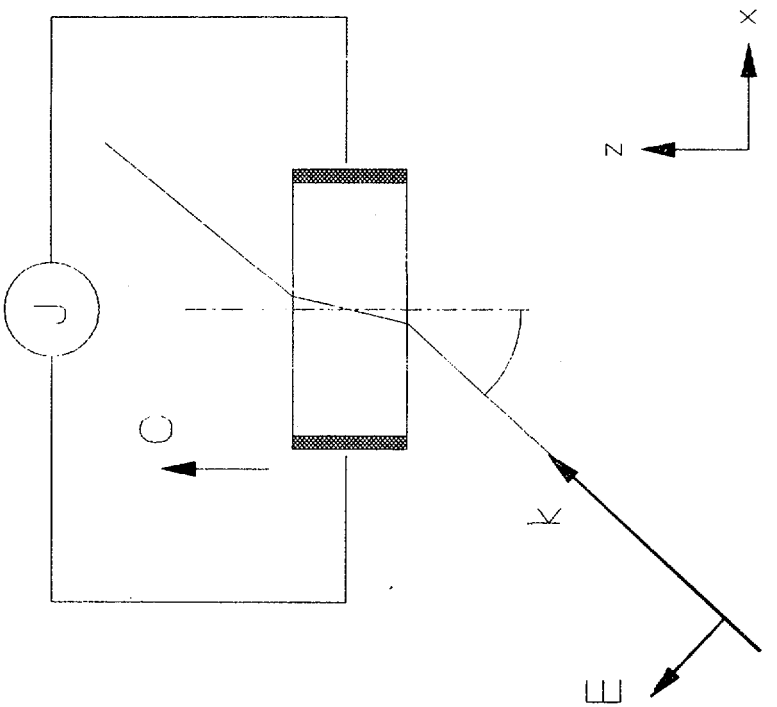

Fig.3

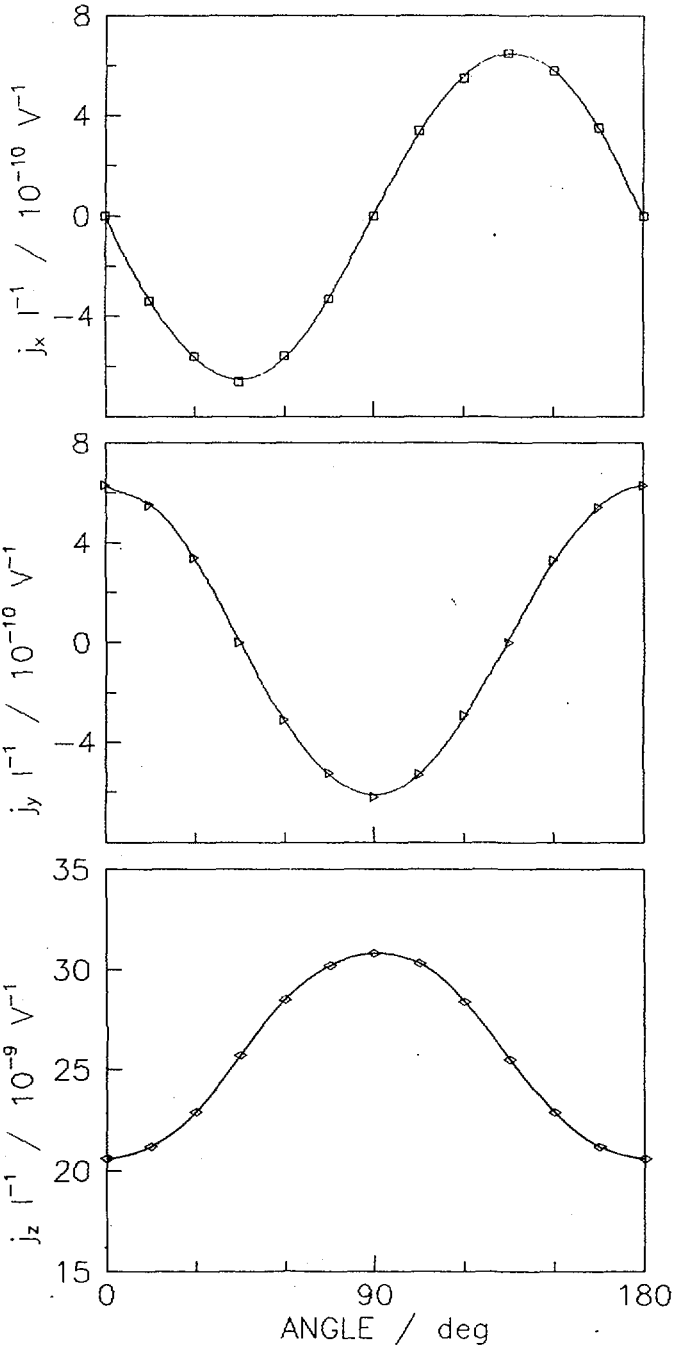
8
4
0
−4
$j_x\ \Gamma^{-1}\ /\ 10^{-10}\ V^{-1}$
8
4
0
−4
$j_y\ \Gamma^{-1}\ /\ 10^{-10}\ V^{-1}$
35
30
25
20
15
$j_z\ \Gamma^{-1}\ /\ 10^{-9}\ V^{-1}$
0
90
180
ANGLE / deg

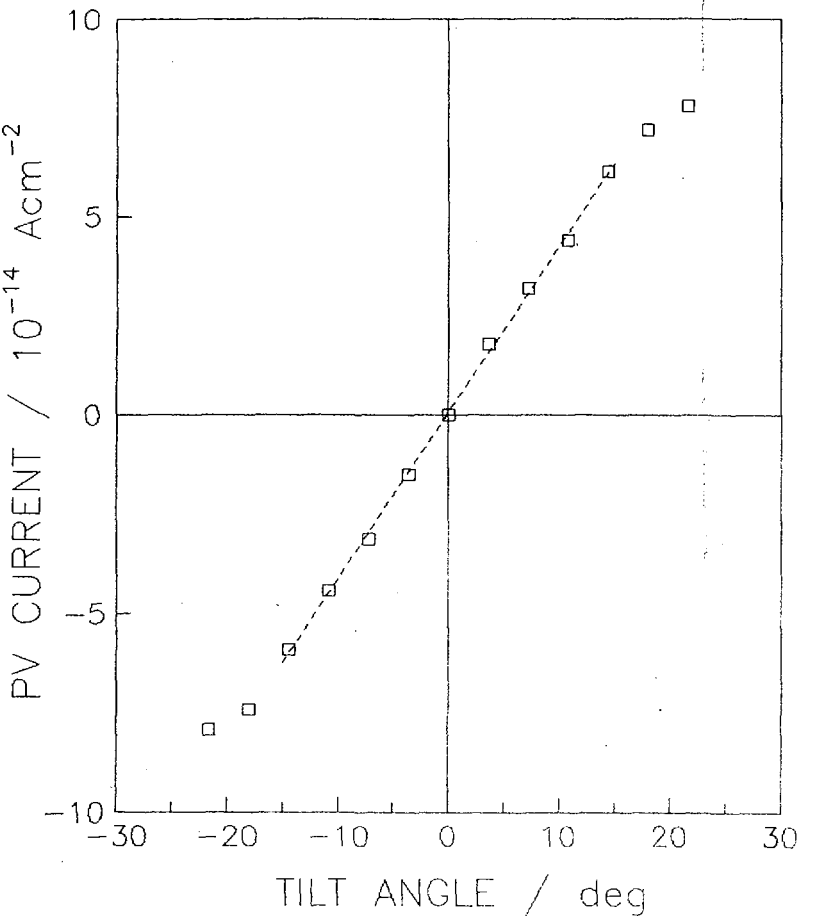

Fig.5

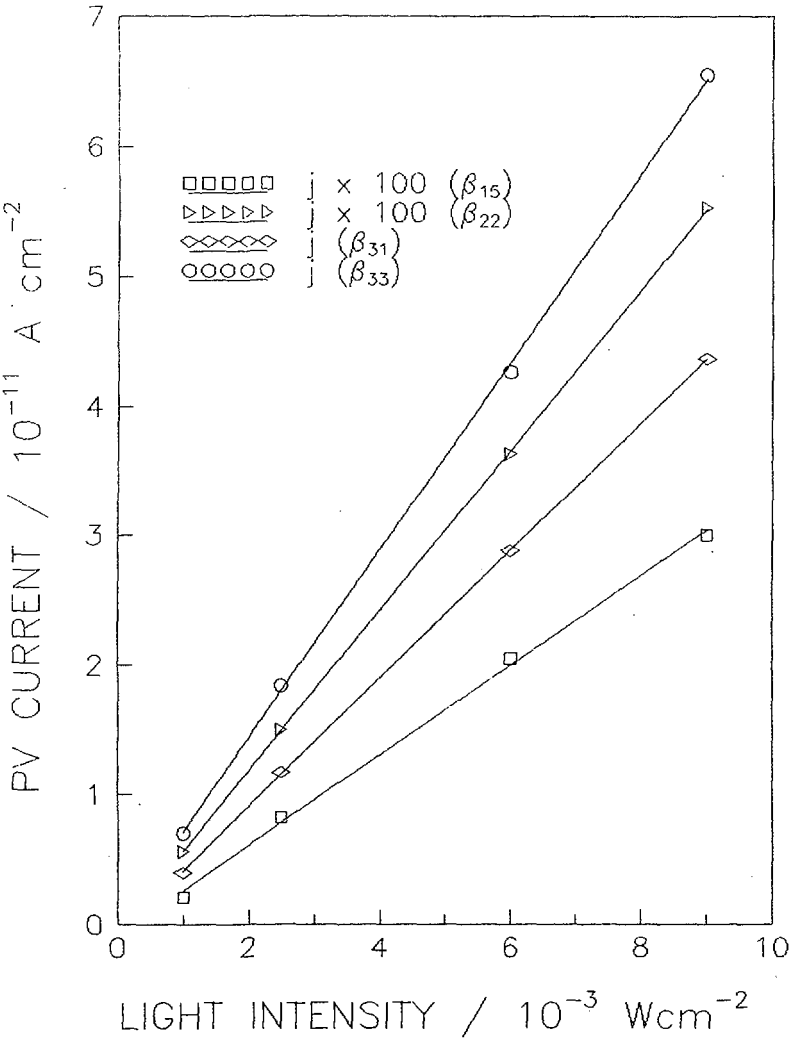
PV CURRENT / 10^{-11} A cm^{-2}
LIGHT INTENSITY / 10^{-3} Wcm^{-2}
0
1
2
3
4
5
6
7
0
2
4
6
8
10
× 100 (β_{15})
× 100 (β_{22})
(β_{31})
(β_{33})

Fig.6

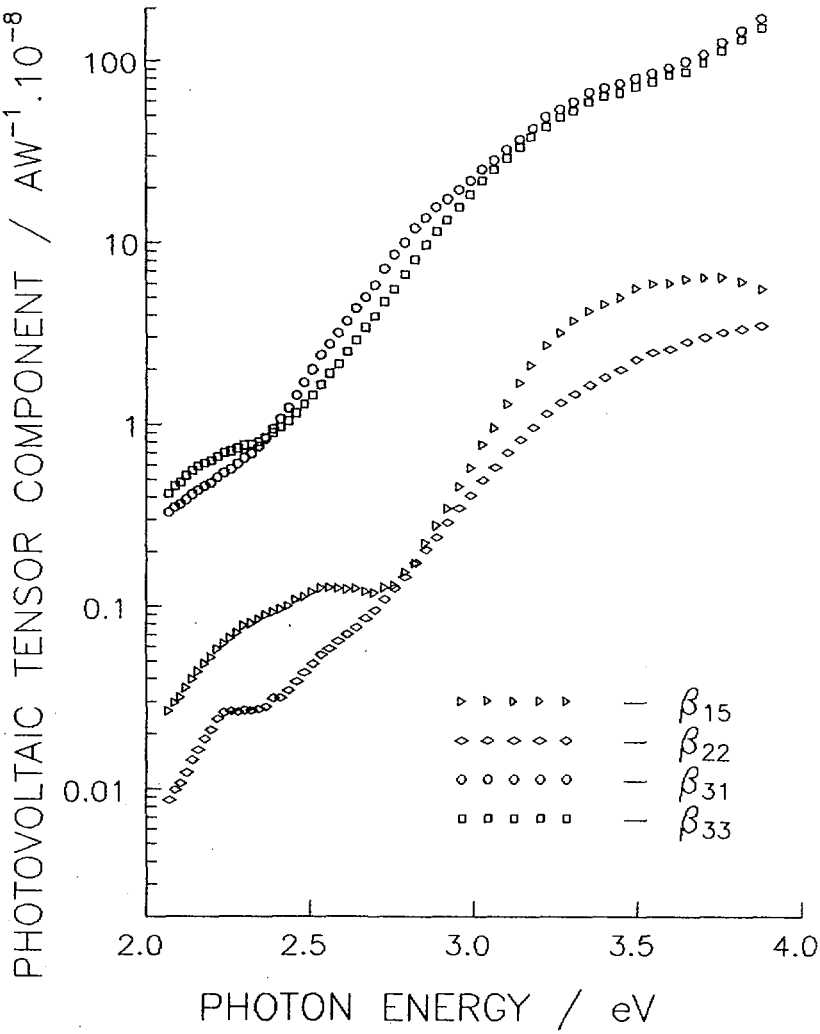
PHOTOVOLTAIC TENSOR COMPONENT / $AW^{-1}.10^{-8}$
100
10
1
0.1
0.01
2.0
2.5
3.0
3.5
4.0
PHOTON ENERGY / eV
β_{15}
β_{22}
β_{31}
β_{33}

Fig.7

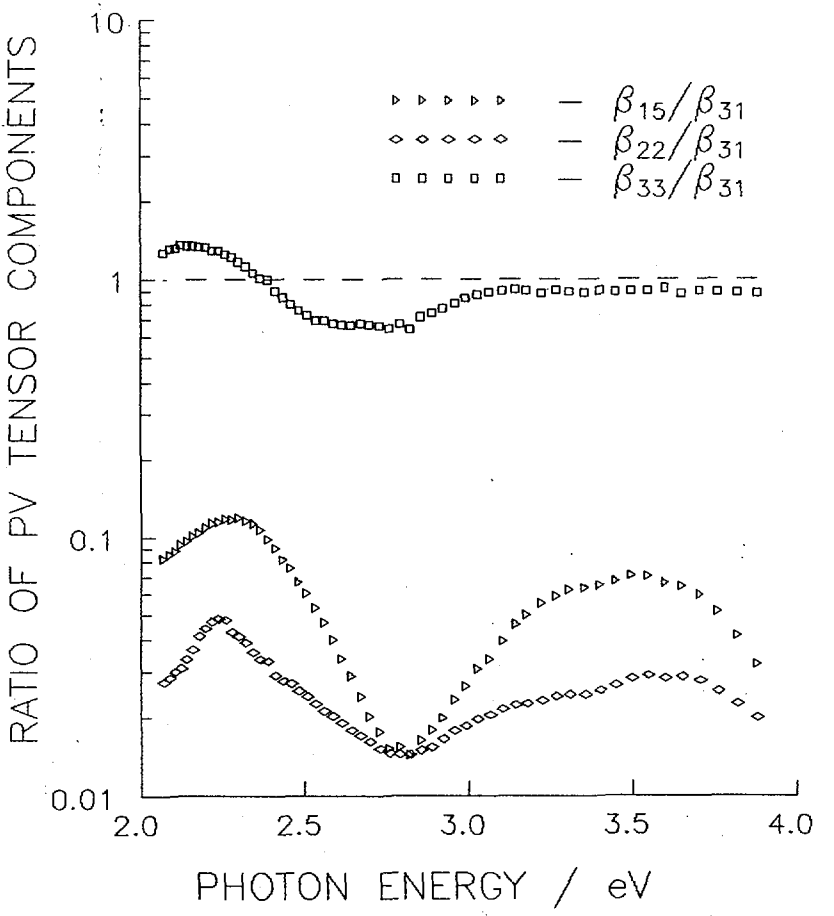
RATIO OF PV TENSOR COMPONENTS
10
1
0.1
0.01
2.0
2.5
3.0
3.5
4.0
PHOTON ENERGY / eV
β15/β31
β22/β31
β33/β31

Fig.8 a

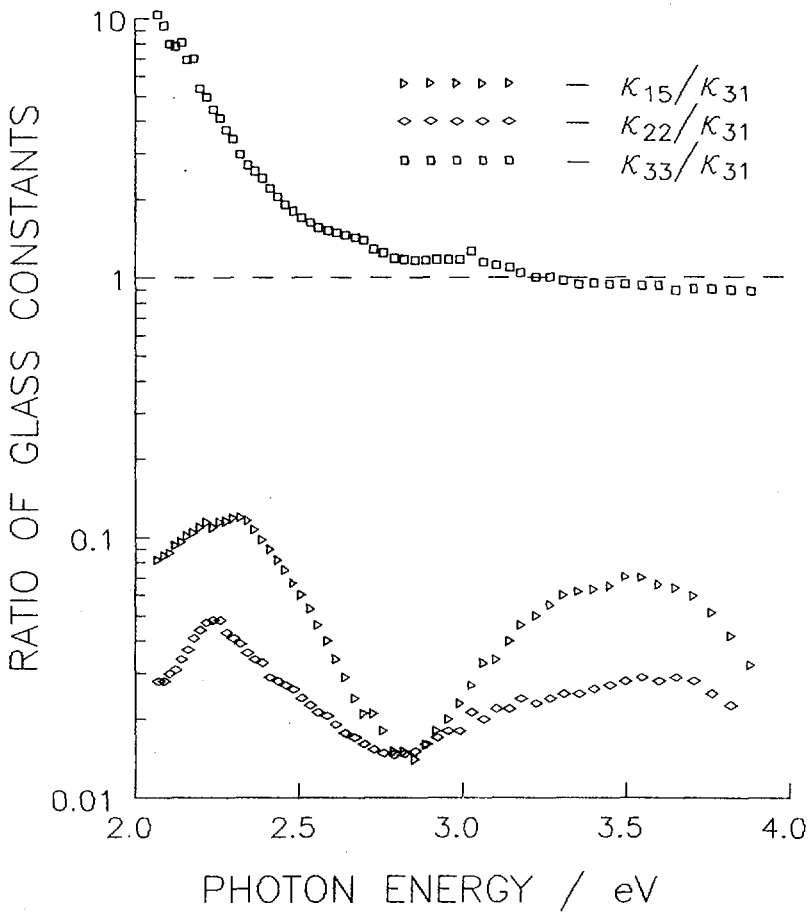
10
1
0.1
0.01
2.0
2.5
3.0
3.5
4.0
RATIO OF GLASS CONSTANTS
PHOTON ENERGY / eV
K_{15}/K_{31}
K_{22}/K_{31}
K_{33}/K_{31}

Fig. 8b

References

[1] A.M.Glass, D. von der Linde, and T.J.Negran, Appl.Phys. Lett. 25, 233 (1974).

[2] V.I.Belinicher, and B.I.Sturman, Usp. fiz. nauk **130**, 415 (1980).

[3] V.M.Fridkin, and R.M.Magomadov, Soviet Phys.- J.exper. theor. Phys., Letters **30**, 723 (1979).

[4] H.G.Festl, P.Hertel, E.Kraetzig, and R. von Baltz, Phys. Status Solidi B **113**, 157 (1982).

[5] S.I.Karabekian, Soviet Phys.- Solid State **33**, 633 (1991).

[6] E.M.Avakian, K.G.Belabaev, and S.G.Odoulov, Izv. AN SSSR (Fizika) **47**, 656 (1983).

[7] E.M.Avakian, K.G.Belabaev, I.N.Kiseleva, S.G.Odoulov, and E.I.Renkachishskaya, Ukr. fiz. Zh. **29**, 790 (1984).

The manuscript was received June 3, 1991

С.И. КАРАБЕКЯН, С.Г.ОДУЛОВ

ОБЪЕМНЫЙ ФОТОВОЛЬТАИЧЕСКИЙ ЭФФЕКТ В КРИСТАЛЛЕ $LiTaO_3$:Fe

(на английском языке, перевод Г.А. Папяна)

Редактор Л.П.Мукаян

Технический редактор А.С.Абрамян

Подписано в печать I6/XII-9Ir. Формат 60×84×16

Офсетная печать. Уч.изд.л. I,0 Тираж 299 экз.Ц.I5 к.

Зак.тип. I80 Индекс 3649

Отпечатано в Ереванском физическом институте

Ереван-36, ул. Братьев Алиханян 2.

The address for requests:
Information Department
Yerevan Physics Institute
Alikhanian Brothers 2,
Yrevan, 375036
Armenia, USSR

ИНДЕКС 3649

ЕРЕВАНСКИЙ ФИЗИЧЕСКИЙ ИНСТИТУТ